Synthesis of Bimetallic Gold-Silver Alloy Nanoclusters by Simple Mortar Grinding

Arumugam Murugadoss, Noriko Kai and Hidehiro Sakurai*

Research Center for Nanoscale Molecular Science, Institute for Molecular Science, Myodaiji,
Okazaki 444 8787, Japan;
E-mail: hsakurai@ims.ac.jp

Experimental details

General: Transmission electron microscope (TEM) and high-resolution TEM (HRTEM) images of Au-Ag and Ag NCs were recorded with a JEOL JEM-3100FE at an accelerating voltage of 300 kV. Typical magnification of the images was 100,000-120,000X. The composition of each individual bimetallic NCs were evaluated using 0.25 nm EDS (energy-dispersive spectrometry) probe in JEOL 3100FE TEM, operating in the bright field scanning transmission electron microscope (BF-STEM) mode. UV-Visible spectra were measured by JASCO V-670 spectrophotometer at 24 °C. Hitachi Temperature controlled U-3500 UV-Vis-NIR spectrophotometer with heating rate of 0.1 °C/min was used to investigate the temperature dependent of kinetics studies of each nanoclusters catalysts. X-ray diffraction pattern of Au-Ag and Ag-Chit was recorded using Rigaku Ultimat III, RINT-2000/PC (Cu Kα radiation under operation at 40 kV and 40 mA), in the powder mode. Inductively coupled plasmon-Atomic emission spectrometry (ICP-AES) of Ag-Chit and Au-Ag NCs was performed by using LEEMAN LABS INC, *Profile plus* with standard calibration samples.

Materials: All chemicals and solvents were used as received without further purification. Hydrogen tetrachloroaurate tetrahydrate ($HAuCl_4$) was obtained from Tanaka Kikinzoku, Chitosan (*poly (D-glucosamine)*) with a medium molecular weight of 75-85 % deacetylated was from sigma Aldrich, and others were obtained from Wako pure chemical industries. Milli-Q grade water was used in all experiments.

Preparation of Ag NCs: The mixture of solid chitosan (0.3 g), $AgNO_3$ (4.3 mg) and NaOH (126 mg) palette were grounded in a mortar at room temperature. The white color mixture became turned into yellow color in a seven minutes and the grinding was further continued for another 13 min. The yellow color powder was washed by membrane filter (pore size 0.05 μm VMWP) in several times until the filtered pH reach to 7. The resulting Ag-chit powder was stored and used for further studies.

Preparation of Au-Ag NCs: The mixture of solid chitosan (0.3g), $AgNO_3$ and NaOH (126 mg) palette were grounded in a mortar at room temperature for seven minutes. The given amount of concentrated $HAuCl_4$ (0.25M) was added into the yellow color powder and the grinding was further continued for 13 min. While grinding the yellow color powder with $HAuCl_4$, the color became changed into dark brown indicating the formation of bimetallic Au-Ag NCs. The powder of chitosan supported Au-Ag NCs was washed by membrane filter and the resulting Au-Ag NCs powder was stored and used for further studies. The final concentrations $AgNO_3$ and $HAuCl_4$ used in these studies are given in the table 1 (See main text).

Ag NCs formation with grinding time: We observed that while grinding $AgNO_3$ with chitosan in the presence of base, the slightly yellow color formed in 2.5 min then the intensity of yellow color further increased with increasing the grinding time (7.5 min). The yellow color is remains unchanged with further increasing the grinding time. The same phenomenon was also observed in the case of Au-Ag NCs formation. Based on the color changes of the metal NCs and our routinely reproducibility results suggests that the longer grinding time does not lead to both cluster size and morphological changes of metal NCs.

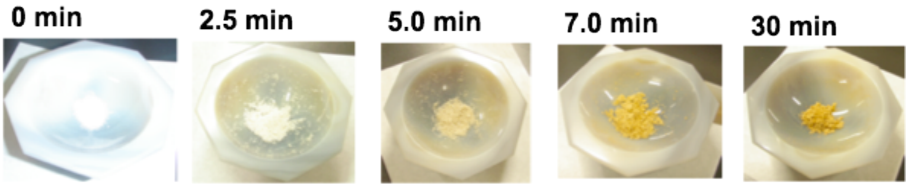

Figure S1. Ag NCs formation with different grinding time.

ICP-AES analysis: The powder Au-Ag and Ag-chit was dissolved into 10 mL aqua regia solution (1:1 aqua regia and water) and were allowed to react at 60 ^oC for over night in order to dissolve the Au and Ag completely. The resulting samples were analysed by ICP-AES.

Preparation of colloidal Ag and Au-Ag NCs: 20 mg of solid chitosan supported Ag or Au-Ag NCs was dissolved in 20 mL aqueous acetic acid (0.02% V/V) solutions and the resulting colloidal solutions was used for further characterization and catalytic studies.

Characterization of Ag-Chit and Au-Ag NCs:

UV-Visible spectroscopy: The UV-Visible spectra colloidal Ag and Au-Ag alloy NCs were performed at room temperature and the sample solutions were not deaerated prior to the measurement.

Transmission electron microscope: A drop of Ag and Au-Ag alloy NCs in water was placed on carbon coated copper grid and followed by air-drying. The drop-coated grid was then analyzed under TEM. The high-resolution TEM images are collected under the magnification of 100.000 -120,0000X

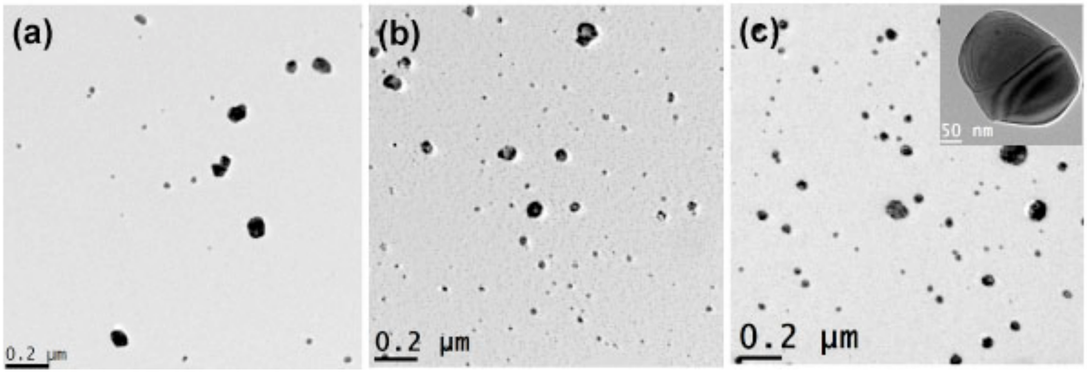

Figure S2. TEM images of larger size silver particles of Cat-1 (a), Cat-2 (b) and (c) Cat-3.

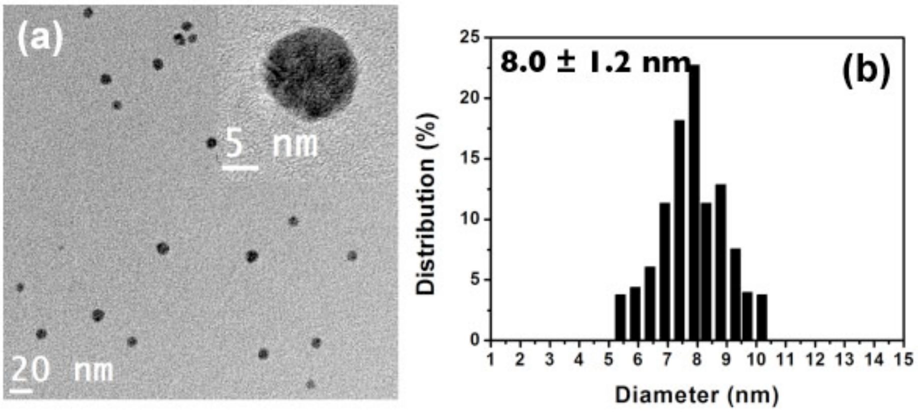

Figure S3. (a) TEM images of Ag-chit and inset figure show the HRTEM image of Ag NCs. (b) Histogram plot of Ag NCs.

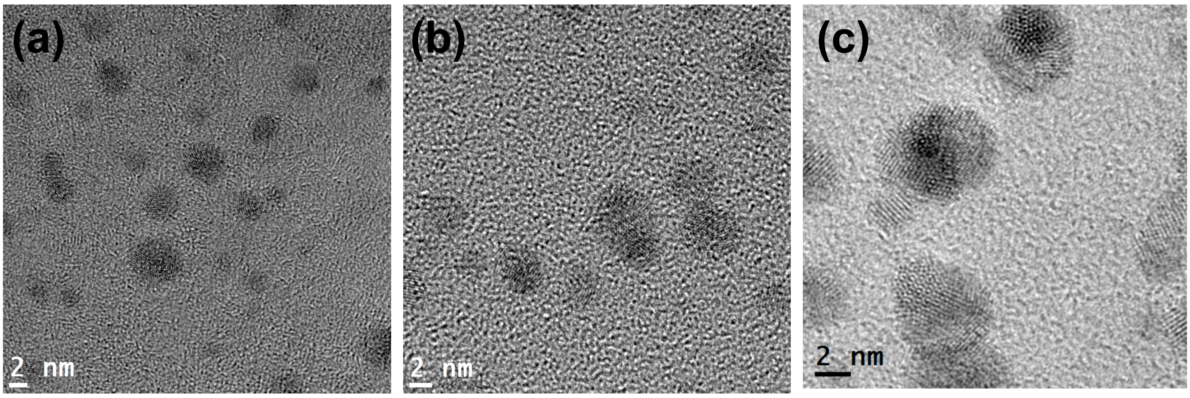

Figure S4. High-resolution TEM images of Cat-1 (a), Cat-2 (b) and (c) Cat-3.

STEM-EDS analysis: The sample grid, which is used for STEM-EDS analysis was same as TEM analysis sample grid. STEM cross sectional composition line profile of in each bimetallic Au-Ag alloy NCs was under bright field mode.

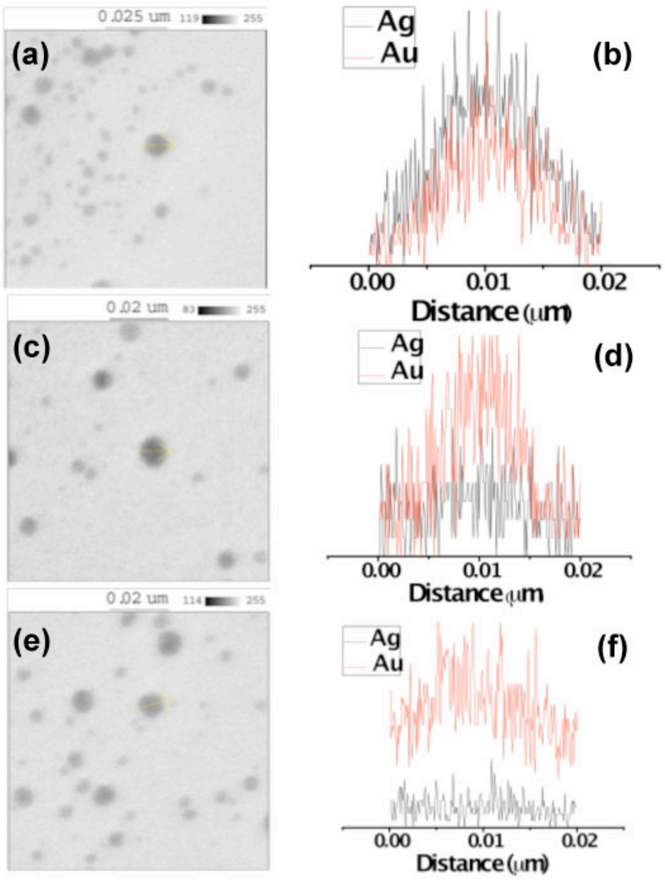

Figure S5. STEM-EDS lines scan EDS spectra across the Au-Ag alloy particles of Cat-1 (a and b), Cat-2 (c and d) and (e and f) Cat-3.

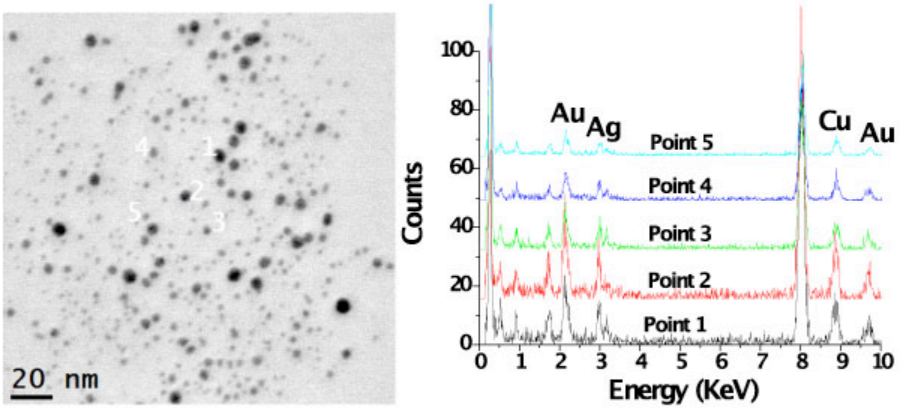

particles	Compositions (%)	
	Ag	Au
point 1	45	55
point 2	40	60
point 3	36	64
point 4	42	58
point 5	56	44

Figure S6. BF-STEM images (left) and the corresponding EDS spectra (right) for the Au-Ag alloy NCs of Cat-1. The copper signal originates from the copper grid. The exact composition of Ag and Au in each Au-Ag NCs are given in the table.

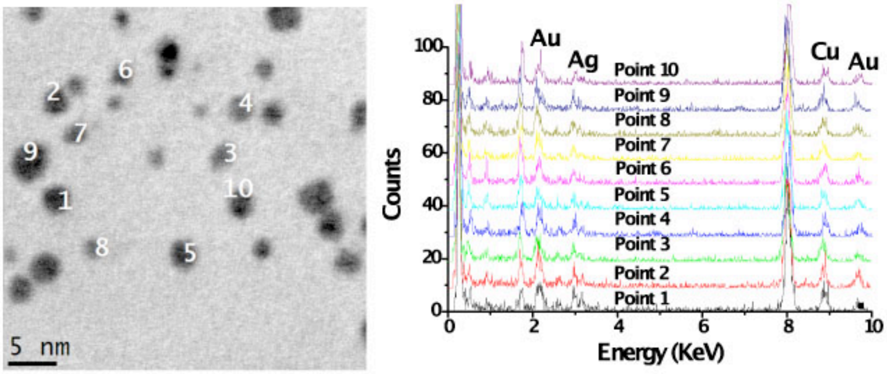

Particles	Compositions (%)	
	Ag	Au
point 1	47	53
point 2	33	67
point 3	32	68
point 4	42	58
point 5	36	64
point 6	35	65
point 7	39	61
point 8	29	71
point 9	48	52
point 10	25	75

Figure S7. BF-STEM images (left) and the corresponding EDS spectra (right) for the Au-Ag alloy NCs of Cat-2. The copper signal originates from the copper grid. The exact composition of Ag and Au in each Au-Ag NCs are given in the table.

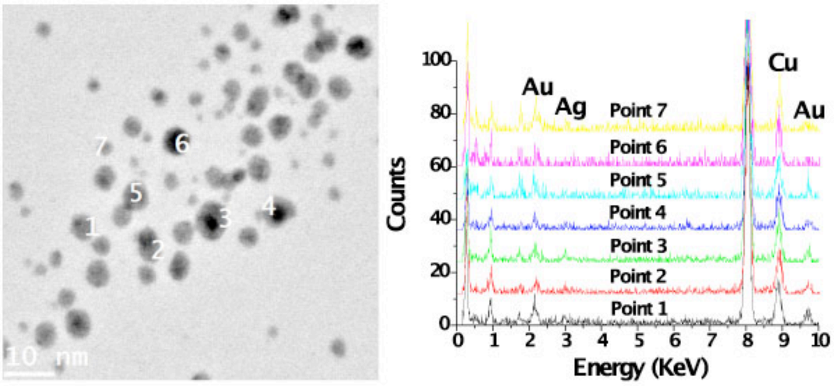

particles	**Compositions (%)**	
	Ag	Au
point 1	17	83
point 2	21	79
point 3	19	81
point 4	21	79
point 5	16	84
point 6	14	86
point 7	20	80

Figure S8. BF-STEM images (left) and the corresponding EDS spectra (right) for the Au-Ag alloy NCs of Cat-3. The copper signal originates from the copper grid. The exact composition of Ag and Au in each Au-Ag NCs are given in the table.

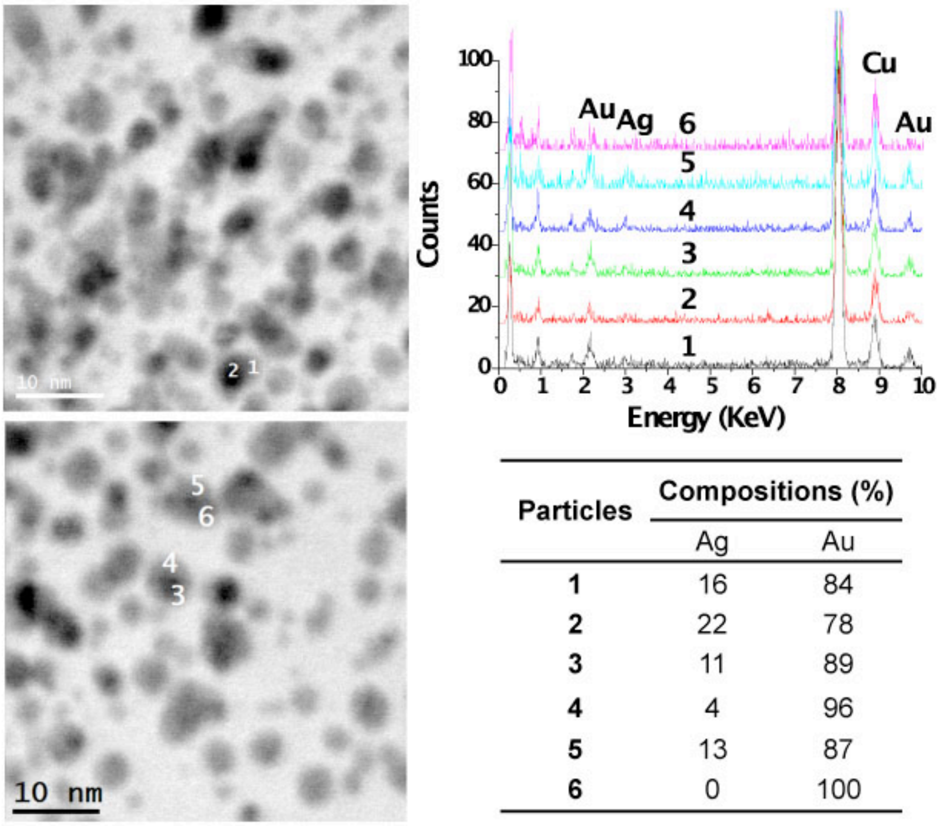

Particles	Compositions (%)	
	Ag	Au
1	16	84
2	22	78
3	11	89
4	4	96
5	13	87
6	0	100

Figure S9. BF-STEM images (left) and the corresponding EDS spectra (right) for the Au-Ag alloy NCs of Cat-3. The copper signal originates from the copper grid. The exact composition of Ag and Au in each Au-Ag NCs are given in the table.

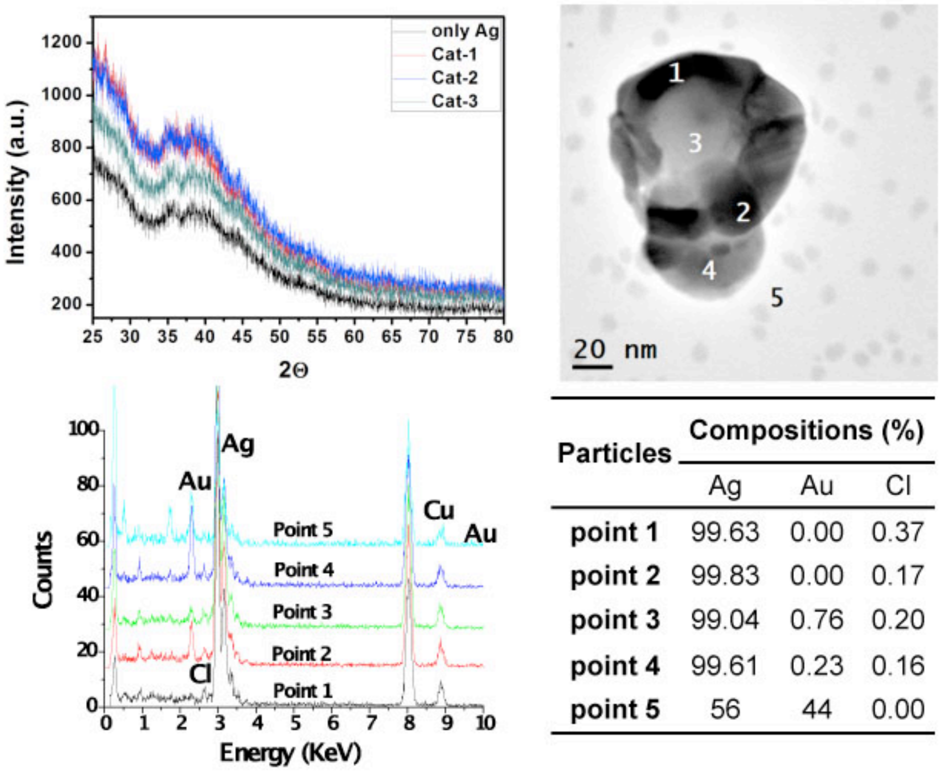

Particles	Compositions (%)		
	Ag	Au	Cl
point 1	99.63	0.00	0.37
point 2	99.83	0.00	0.17
point 3	99.04	0.76	0.20
point 4	99.61	0.23	0.16
point 5	56	44	0.00

Figure S10. X-ray diffraction pattern of Ag and Au-Ag NCs (left). BF-STEM images (right) and the corresponding EDS spectra (left) for the Au-Ag alloy NCs of Cat-2. The copper signal originates from the copper grid. The exact composition of Ag and Au in the bigger particles is given in the table. These results demonstrate that the whole bigger size particles are composed only silver atoms.

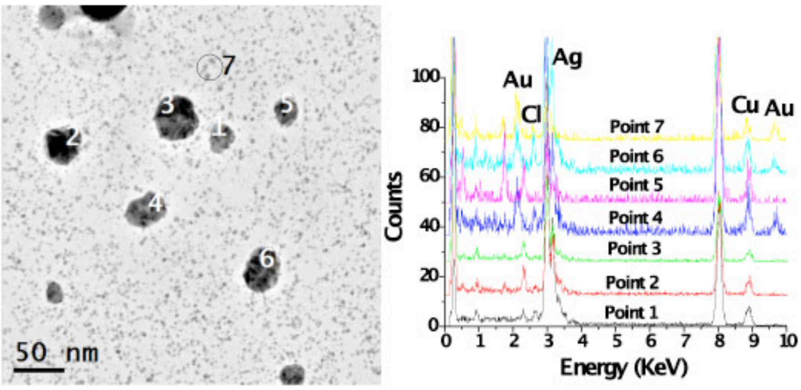

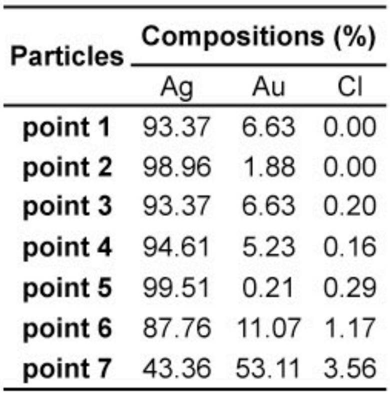

Particles	Compositions (%)		
	Ag	Au	Cl
point 1	93.37	6.63	0.00
point 2	98.96	1.88	0.00
point 3	93.37	6.63	0.20
point 4	94.61	5.23	0.16
point 5	99.51	0.21	0.29
point 6	87.76	11.07	1.17
point 7	43.36	53.11	3.56

Figure S11. BF-STEM images (left) and the corresponding EDS spectra (right) for the Au-Ag alloy NCs of Cat-2. The copper signal originates from the copper grid. The exact composition of Ag and Au in each Au-Ag NCs are given in the table.

Catalytic studies:

Typically, in a 3 mL quartz cell, 2.5 mL of freshly prepared 10mM of $NaBH_4$ solution and 25 µL of 10 mM of 4-nitrophenol solutions was added. The molar ratio of 4NP and $NaBH_4$ was maintained 1:100 throughout all the catalytic reactions. To this mixture, a specific amount of chitosan supported Ag and Au-Ag NCs catalysts (20-70 µL) was added. The mixture was shaken once for thorough mixing and then kept in the sample compartment of a UV-Vis spectrophotometer. UV-visible absorbance spectra were recorded over time to monitor the change in the reaction mixture. All the catalytic studies were performed at 27 ^{o}C.

Temperature dependent kinetics studies: The catalytic reaction of 4-NP was studied at five different temperatures (10, 20, 30, 40 and 50 °C). The rate of the reaction was calculated for the different temperatures for the Ag and Au-Ag NCs as the catalysts. The apparent activation energy of the Ag and each Au-Ag alloy NCs catalysts was obtained from the Arrhenius rate equation.[1-3] The activation energies of each catalyst were summarized in table S2.

Reduction of other nitroarenes: 3mM of nitroarenes (4.2 mg of 2-nitroaniline, 2-nitrophenol and 4-nitraniline) was added into 10 mL of freshly prepared aqueous $NaBH_4$ (0.3M) solutions. The mixture was stirrer at 900 rpm at 27 °C. To this mixture, 10 mg of Cat-1 was added and the stirring was continued. The reaction progress was monitored with UV-Visible absorbance spectra by assessing the small portion of the reaction mixture at regular time interval (3 min). The absorbance spectra of solutions were measured in the range of 250-500 nm. The observed results were compared with the previously reported results[4-6] indicating that Au-Ag NCs of Cat-1 could able to catalyze the reduction of various nitroarnes substrates.

Procedure for the reuse of Au-Ag alloy catalysts: The reusability of Cat-1 was checked by reduction of 4NP. The procedure was same as with the reduction of other nitroarene substrates. After completion of the reaction, the catalysts were easily separated by through the membrane filter, and then washed with water several times (preferably more than 4 times). Thus-recovered Au-Ag NCs of Cat-1 were transferred to the reaction test tube to run for the next cycle.

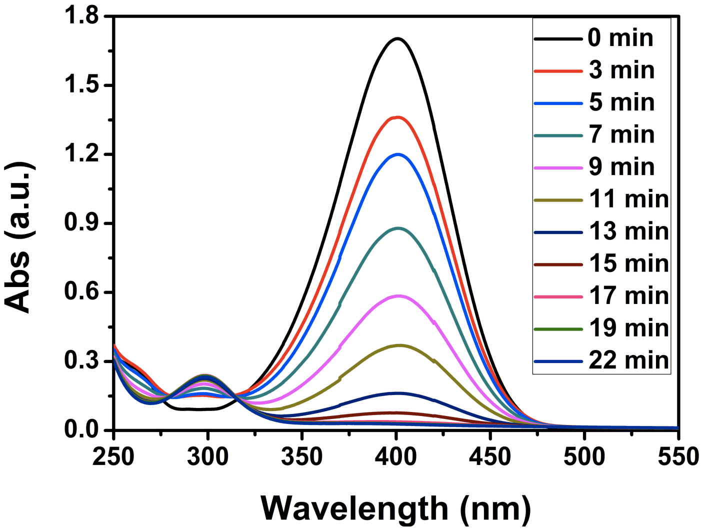

Figure S12. The absorbance spectra of 4NP at different time intervals in the presence of Ag NCs. The concentration of Ag NCs was 2.70 μM.

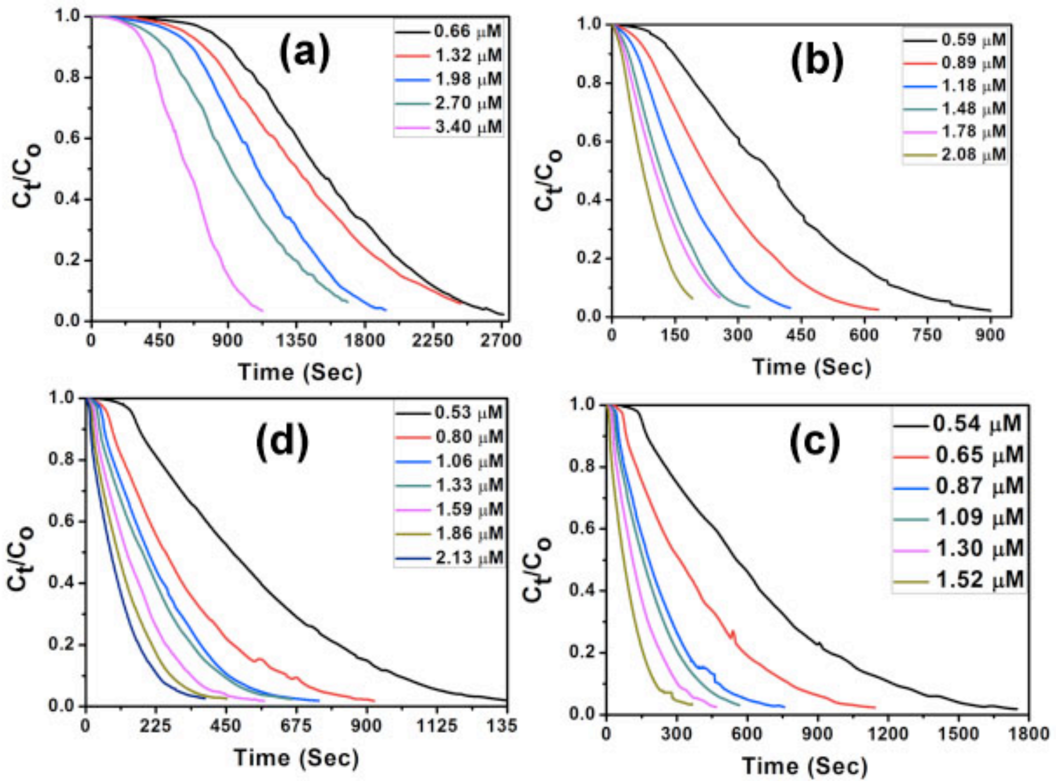

Figure S13. The normalized absorption decay of 4NP with time over different catalysts. (a) Ag NCs, (b) Cat-1, (c) Cat-2 and (d) Cat-3. The concentration of each nanoclusters catalysts is indicated in the panel of each figure.

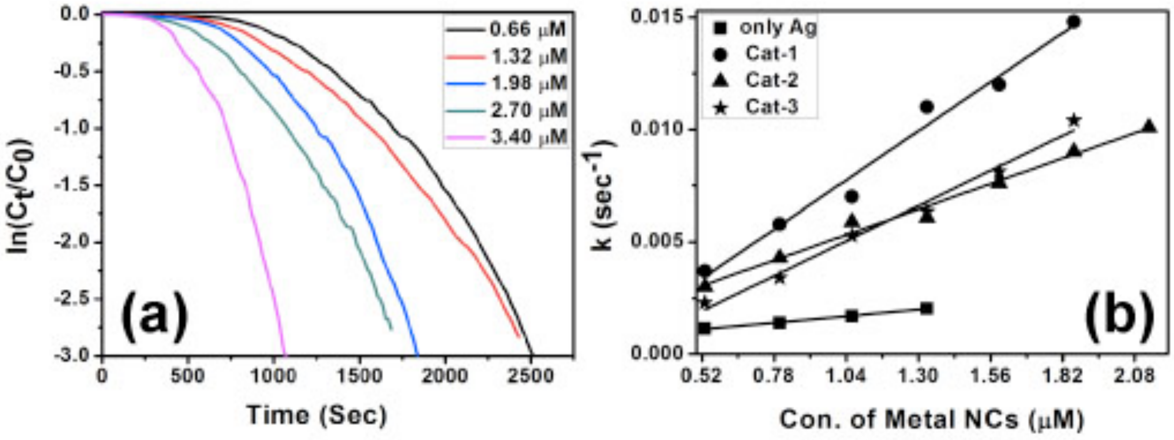

Figure S14. (a) Plots of $\ln(C_t/C_o)$ versus time over Ag NCs catalysts. (b) The reaction rate constants with function of total metal concentration per unit volume in each nanocluster catalysts.

***Table S1**. Rate constants and apparent activation energy of Ag, Cat-1, Cat-2 and Cat-3.*

	only Ag	**Cat-1**	**Cat-2**	**Cat-3**
Rate constants, k ($S^{-1}.M^{-1}$)	1.11X10^{1}	8.45 X10^{3}	6.0 X10^{3}	4.35 X10^{3}
Activation Energy, E (k.j/mol)	113	27	42	58

Reduction of other nitroarenes:

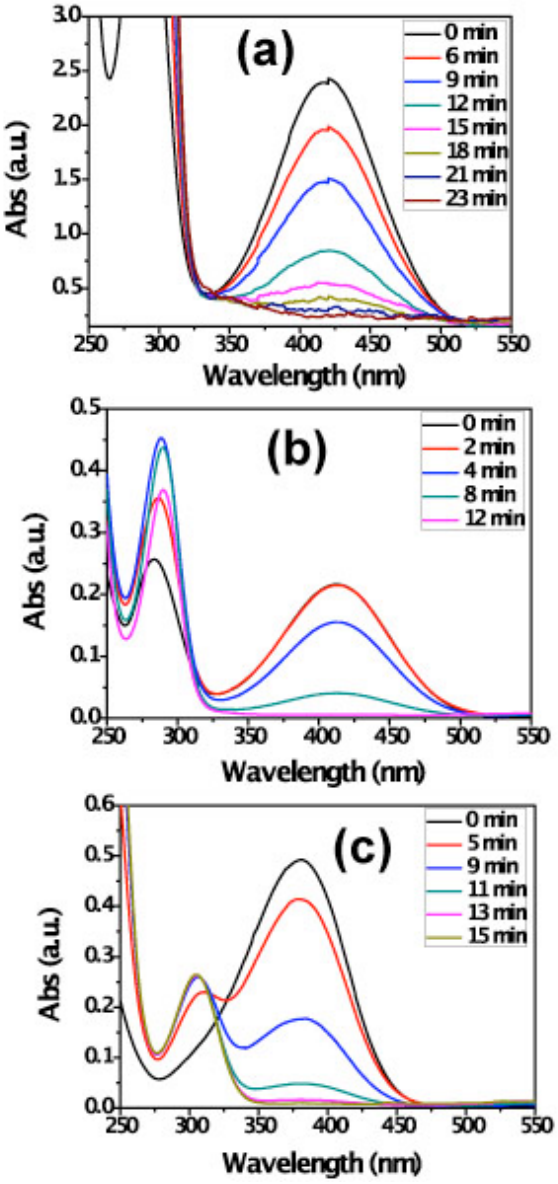

Figure S15. Au-Ag alloy NCs of cat-1 catalyzed reduction of 2-nitrophenol (a), 2-nitroaniline (b) and 4-nitroaniline (c). The amount of catalyst was 10 mg of Cat-1.

Reusability test:

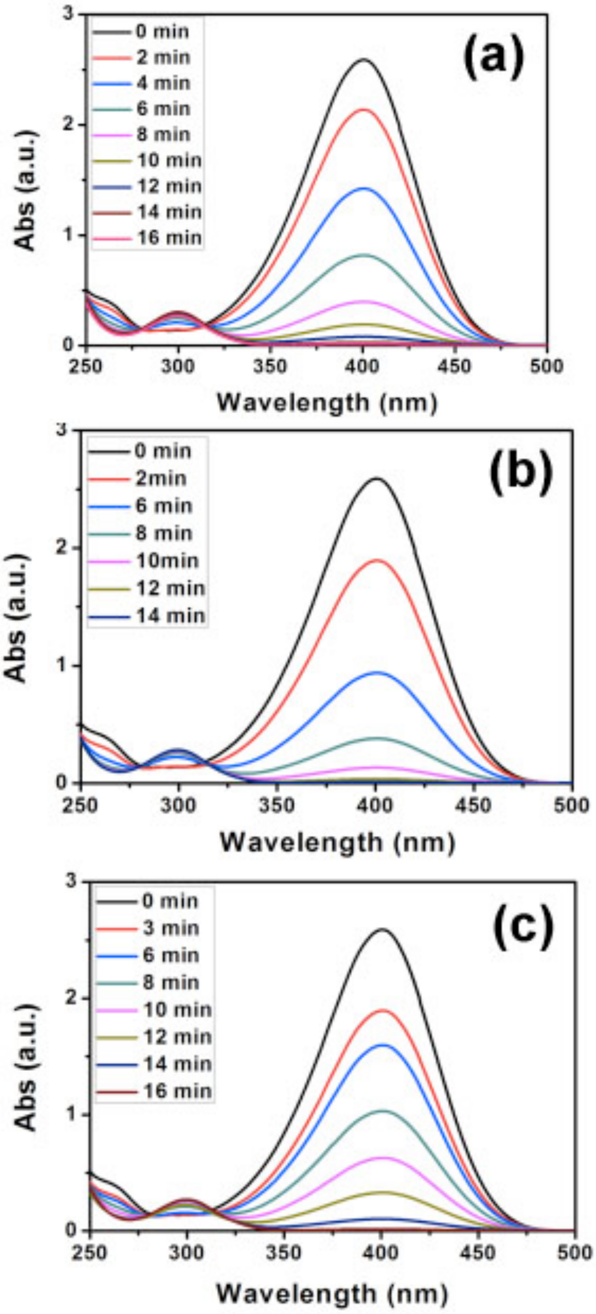

Figure S16. The absorption spectra of 4NP at different time interval (a) 1st, (b) 2nd and (c) 3rd runs of the catalytic reduction of 4NP over Au-Ag alloy NCs of Cat-1.

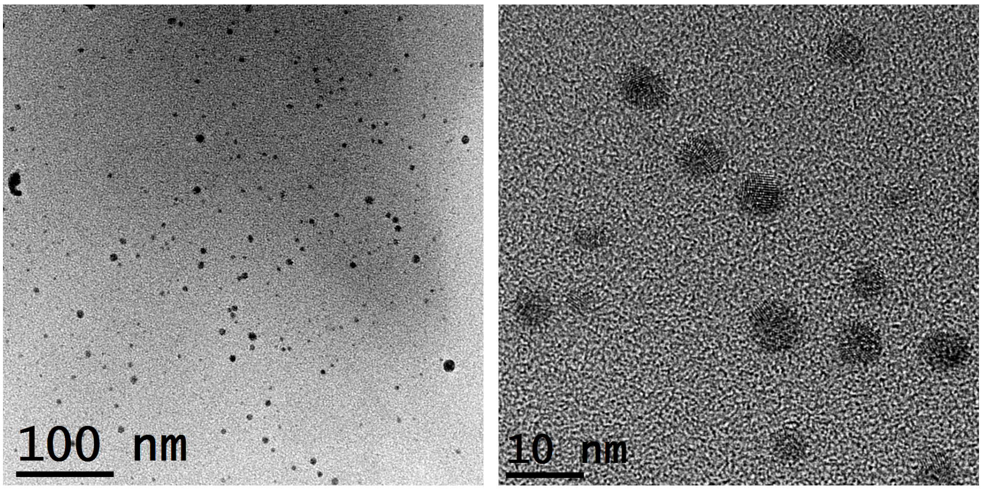

Figure S17. TEM and HRTEM images of Au-Ag alloy NCs of Cat-1 after 3rd cycle.

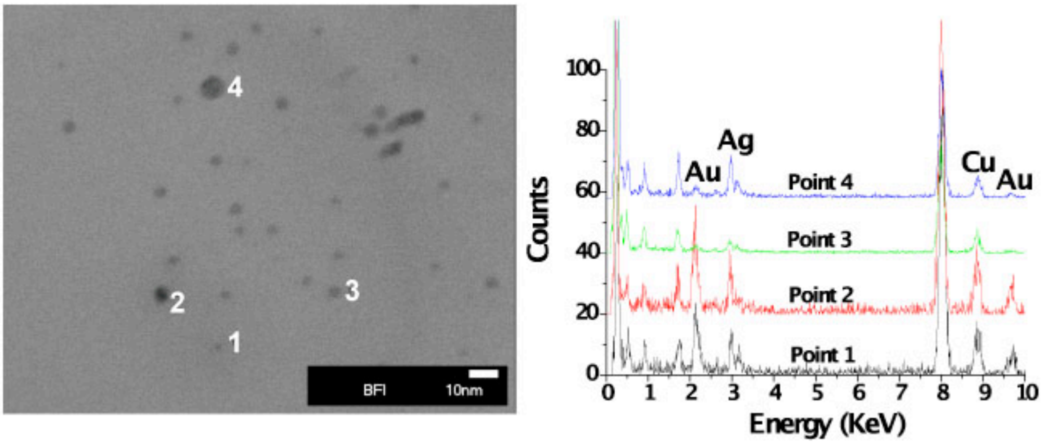

Particles	Compositions (%)	
	Ag	Au
point 1	68	32
point 2	56	44
point 3	70	30
point 4	34	66

Figure S18. BF-STEM images (left) and the corresponding EDS spectra (right) for the Au-Ag alloy NCs of Cat-1 after third cycle. The copper signal originates from the copper grid. The exact composition of Ag and Au in each Au-Ag NCs are given in the table.

References

1. Y. Lu, Y. Mei, M. Drechsler and M. Ballauff, *Angew. Chem. Int. Ed.,* 2006, **45**, 813-816.

2. M. A. Mahmoud, F. Saira, and M. A. El-Sayed, *Nano Lett.,* 2010, **10**, 3764-3769.

3. S. Saha, A. Pal, S. Kundu, S. Basu, T. Pal, *Langmuir*, 2010, **26**, 2885–2893.

4. S. Kundu, K. Wang, and H. Liang, *J. Phys. Chem. C,* 2009, **113**, 5157-5163.

5. Y. Yong, S.Yan, H. Ying and Y. Chaoguo, *Chin. J. Chem.,* 2010, **28**, 705-712.

6. J. Huang, L. Zhang, B. Chen, N. Ji, F. Chen, Y. Zhang and Z. Zhang, *Nanoscale,* 2010, **2**, 2733-2738.
